

# Adaptive and Collaborative Bathymetric Channel-Finding Approach for Multiple Autonomous Marine Vehicles

Nikolai Gershfeld<sup>1</sup>, Tyler M. Paine<sup>1,2</sup> and Michael R. Benjamin<sup>1</sup>

**Abstract**—This paper reports an investigation into the problem of rapid identification of a channel that crosses a body of water using one or more Unmanned Surface Vehicles (USV). A new algorithm called Proposal Based Adaptive Channel Search (PBACS) is presented as a potential solution that improves upon current methods. The empirical performance of PBACS is compared to lawnmower surveying and to Markov decision process (MDP) planning with two state-of-the-art reward functions: Upper Confidence Bound (UCB) and Maximum Value Information (MVI). The performance of each method is evaluated through comparison of the time it takes to identify a continuous channel through an area, using one, two, three, or four USVs. The performance of each method is compared across ten simulated bathymetry scenarios and one field area, each with different channel layouts. The results from simulations and field trials indicate that on average multi-vehicle PBACS outperforms lawnmower, UCB, and MVI based methods, especially when at least three vehicles are used.

## I. INTRODUCTION

Autonomous marine vehicles are important tools for many applications in both civilian and military contexts. One such application is Rapid Environmental Assessment (REA), where a vehicle provides information about the physical environment in an area of interest. This information is then used to inform future missions. In a riverine environment with unknown bathymetry, this can entail quickly identifying a channel that can provide a navigable path through the area. We refer to this as the rapid channel identification problem. This paper will focus on the development of a new algorithm to efficiently address this problem. We compare this new method to other state-of-the-art approaches and investigate the utility of using multiple vehicles in the solution.

The simplest way to survey an area is with a lawnmower search pattern. This is the most exhaustive method and will provide a comprehensive overview of the environment. However, for this problem we are interested in finding a specific feature – a deep channel – rather than constructing a complete map. To speed up this process, we can employ *adaptive* sampling strategies. This terminology refers to a broad class of algorithms where a robot updates its sampling strategy according to real-time observations.

Using adaptive sampling and multi-vehicle task allocation techniques, we present the Proposal Based Adaptive Channel

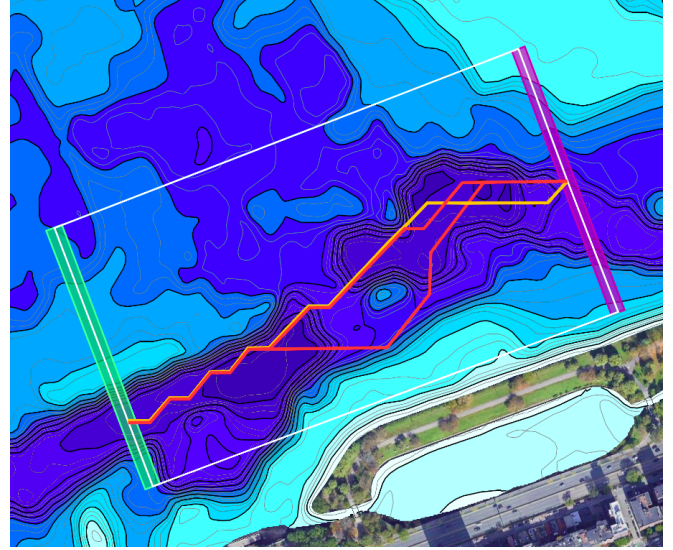


Fig. 1. Viable paths found through the channel in the Charles River using the PBACS algorithm. The rapid channel identification problem involves finding a deep path that connects the start (green) and goal (magenta) regions. A team of two to three Heron USVs identified these viable paths - shown as red and yellow traces - through the deep trench present in the Charles River near MIT campus. The red lines mark paths found with a minimum depth of 22 feet, and the yellow line marks paths found with a minimum depth of 23 feet. The bathymetry map data was provided by the Charles River Alliance of Boaters [1]

Search (PBACS) algorithm for rapid channel identification. We also compare its performance with that of three other sampling methods, and compare their performance when using different numbers of vehicles. The four approaches we tested were:

- 1) Proposal Based Adaptive Channel Search (PBACS)
- 2) Lawnmower survey
- 3) Markov decision process with Upper Confidence Bound (UCB) reward
- 4) Markov decision process with Maximum Value Information (MVI) reward

We compare the methods by testing them against ten different bathymetry maps. Through this testing, we aim to identify a strategy that will work consistently well for different bathymetry configurations.

## A. Contributions and Overview

The contributions of this research are the following:

- The PBACS algorithm, a new specialized method for solving the rapid channel identification problem

\*This work was supported by the United States Military Academy at West Point and the Office of the Undersecretary of Defense for Research and Engineering (ACC-APG-RTP W911NF2120206)

<sup>1</sup>Dept. of Mechanical Engineering, Massachusetts Institute of Technology, Cambridge, Massachusetts, USA gersni@mit.edu, tpaine@mit.edu, mikerb@mit.edu

<sup>2</sup>Applied Ocean Science and Engineering, Woods Hole Oceanographic Institution, Woods Hole MA, USA

- Application of a myopic MDP planner to the rapid channel identification problem
- Comparison of the utility of using different amounts of vehicles in a channel finding mission for the different path planning approaches
- Field deployment of the MDP approaches using up to three USVs, and deployment of the PBACS approach using up to four USVs.

The remainder of the paper is organized as follows. In Section II, we provide a brief overview of related work on marine adaptive sampling and multi-vehicle collaboration. In Section III, we present our approach - the PBACS algorithm - and discuss alternatives. In Section IV, we provide the experimental methods used in simulation and fieldwork studies as well as the results. Finally, in Section V we summarize and conclude.

## II. LITERATURE REVIEW

A robot is considered to be *adaptively* sampling when the sampling strategy is adjusted in real time during the mission, based on the data being collected. Adaptive sampling typically requires two main layers: field estimation, usually with Gaussian processes, and path planning. There are also at least three major classes of adaptive systems problems: source localization, front/boundary determination, and feature tracking and mapping. Furthermore, sampling with multiple vehicles often requires additional strategies for optimized performance. The remainder of this section summarizes previous research in these areas, with an emphasis on fielded systems for marine applications.

### A. Gaussian Processes and Path Planning

In order to effectively make decisions and adjust its path, the vehicle needs to store past measurements and assemble a model of the environment. This can be achieved using Gaussian processes (GP) [2], which are used to represent a probability distribution over functions. Gaussian process regression (GPR), also referred to as kriging, can be used to estimate the mean and covariance values for a set of inputs in the domain.

Gaussian processes are frequently used in marine adaptive sampling for spatial modeling of the estimated environment. Berget et al. [3] use GP methods to track suspended material plumes. The model is updated continuously throughout the mission, and the path planner uses this estimation to drive the unmanned vehicle to information-rich areas. In Fossum et al. [4], GP modeling is used for adaptive sampling of phytoplankton by modeling the distribution of chlorophyll-a - a common indicator of phytoplankton activity. Yan et al. [5] use GPR analysis to guide online path planning for an AUV in an effort to locate hotspots in the field. Another work to use GP methods is Stankiewicz et al. [6], where an AUV uses adaptive sampling to explore an area and identify hypoxic zones. The algorithm identifies regions of interest that exhibit some local extrema and concentrates sampling there.

### B. Classes of Adaptive Sampling Problems

Prior work in marine adaptive sampling can be separated into three broad categories: source localization, front/boundary determination, and feature tracking and mapping. Of these categories, the channel-finding problem explored in this paper is most closely related to the last.

Adaptive source localization, also called maximum seek and sample, is a problem adjacent to the channel-finding problem. Bayat et al. [7] offer a survey of techniques that have been employed in solving this problem. One is gradient based, such as the approach reported by Paliotta et al. in [8]. Another approach, proposed and tested by Flaspohler et al. [9], uses a partially observable Markov decision process (POMDP) with a reward based on maximum value information (MVI), originally developed by Wang et al. [10].

The second category is front or boundary estimation. Examples of this can be found in [11] and [12], where an AUV moves in a vertical sawtooth trajectory to detect and track a front. Fiorelli et al. [13] also address this type of problem using adaptive formations of multiple gliders to identify the cold boundaries in Monterey Bay.

The closest category to the problem explored in this paper is adaptive feature mapping and tracking. An example of a work in this category is Bennett et al. [14], where a simulated AUV is used to adaptively map bathymetric features such as trenches or specific contours.

### C. Multi-Vehicle Considerations

Multi-vehicle systems provide advantages, but can incur additional costs due to increased complexity that must be addressed. When using multiple vehicles for sampling, there are a number of considerations, including vehicle placement, information sharing, and task allocation.

1) *Vehicle placement*: One of the main considerations in multi-vehicle missions is their formation. When the vehicles all explore the entire field, they can be in fixed formations such as in a leader-follower strategy employed by Khoshrou et al. [15] and Paliotta et al. [8], or more flexible approaches such as generating different sailing directions for each vehicle, as proposed by Yan et al. in [5]. When the field is explicitly divided, the divisions can either be predetermined or dynamic. An example of the latter is Kemna et al. [16], where dynamic Voronoi partitioning is used to divide the field among a group of AUVs.

2) *Information sharing and consensus*: To be effective collaborators, vehicles must fuse their information with that of their neighbors to gain a more complete understanding of the field. These communications can be range restricted, especially in the marine domain. Consensus protocols and algorithms have been researched for multi-vehicle coordination across domains [17], [18]. One direction proposed by Ren et al. [19], motivated by Kalman filters, is a Kalman consensus that accounts for the relative confidence of each vehicle's information. A modified version of this algorithm was later developed by Alighanbari et al. [20] which removes potential biases that occur when the agents in the network are not fully connected.

3) *Task allocation*: In many cases, vehicles need to coordinate new tasks/roles that arise as the mission progresses. One class of algorithms for solving this problem of task allocation is auction-based algorithms, also referred to as market-based algorithms. The implementations of these algorithms can rely upon a centralized repository, as described by Bertsekas [21], or they can be distributed, as described by Michael et al. [22] and Zavlanos et al. [23]. In the distributed case, the vehicles can perform the auction only with its neighbors, which would avoid failure if a vehicle drops out of communications range temporarily. In this case, a secondary step can be appended to the distributed auction-based algorithm, which is a consensus protocol to resolve conflicts and improve global performance [24], [25].

### III. METHODOLOGY

This section details the architecture of our distributed autonomous multi-vehicle approach. We begin by describing how the problem is modeled, then explain how a local environmental model is generated in real-time from the sensor data. We discuss how all local models are shared and combined among the fleet using a distributed consensus protocol. Finally, we describe the decentralized PBACS algorithm which operates using the fleet-wide consensus estimate of the environment model.

We represent the bathymetry data in a discrete set of  $m$  grid-cells. We define the vectors  $\vec{z} \in \mathbb{R}^m$  and  $\vec{\sigma} \in \mathbb{R}_+^m$  as the depth and the variance (respectively) of each cell. The location of the center of the  $i^{th}$  cell is denoted as  $\vec{x}_i \in \mathbb{R}^2$

#### A. Single-Beam Depth Sensor

We assume the depth directly below each vehicle can be measured by a single-beam acoustic depth sensor. For field work, we used the Ping Sonar Altimeter and Echosounder made by Blue Robotics for its low cost and commercial availability. A simulated sensor with comparable accuracy and noise was used for simulation studies.

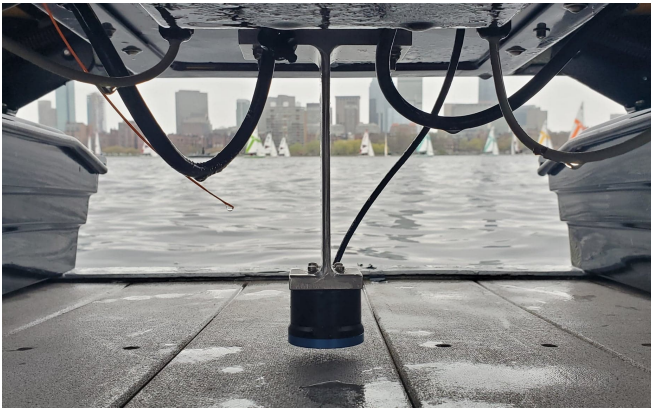


Fig. 2. Altimeter mounted onto the bottom of a Heron vehicle. The Heron USVs are made by Clearpath Robotics

The sensor was mounted onto the bottom plate of each Heron USV the lowest possible depth so that it remains submerged at all times without contacting the dock. The

sensor was mounted directly below the GPS sensor in order to ensure that the distance readings are associated with the correct position. The sensor was then connected to the Heron's payload autonomy computer and integrated into the MOOS system described in Section III-D. We set the sampling rate of the sensor to 10 Hz.

#### B. Gaussian Process Regression

We use GPR on each vehicle to calculate an estimate for the bathymetry field from the collection of local measurements. The GPR implementation used in this system is adapted from the "Fast GPR" developed by Das et al. [26]. The Fast GPR aims to speed up computation by developing estimators on subsets of the dataset. Using the standard implementation of GPR on a dataset of size  $N$  yields  $O(N^3)$  time complexity. By choosing  $k$  subsets of size  $N_s < N$ , the time complexity of Fast GPR is reduced to  $O(kN_s^3)$ . One limitation of this method is that the variance becomes skewed, but this can be addressed by rescaling.

We use the radial basis function kernel

$$\mathcal{K}(\vec{x}_i, \vec{x}_j) = \exp\left(-\frac{d(\vec{x}_i, \vec{x}_j)}{2l^2}\right), \quad (1)$$

where  $d(\vec{x}_i, \vec{x}_j)$  is the Euclidean distance. We determined experimentally that  $l^2 = 830 ft$  works well in field testing.

#### C. Kalman Consensus

For our multi-vehicle coordination, we use the Modified Decentralized Kalman Consensus (MDKC) reported by Alighanbari and How [20]. Estimates from all vehicles are combined through iterative rounds in the consensus process. A consensus can be reached even if the group does not form a fully connected graph, which happened periodically during field operations as vehicles temporarily drop out of communication. A consensus manager was developed to manage requests, iterations, and timeouts. An instance of the manager runs on every vehicle to achieve fully decentralized estimation.

For  $n$  agents  $\mathcal{A} = \{\mathcal{A}_i, \dots, \mathcal{A}_n\}$ , the solution for an agent  $\mathcal{A}_i$  at time  $t + 1$  is given by:

$$\begin{aligned} \mathbf{P}_i(t+1) = & \{[\mathbf{P}_i(t) + \mathbf{Q}(t)]^{-1} \\ & + \sum_{j=1}^n (g_{ij}(t) [\mu_j(t) \mathbf{P}_j(t)]^{-1})\}^{-1} \end{aligned} \quad (2)$$

$$\begin{aligned} \vec{z}_i(t+1) = & \vec{z}_i(t) \\ & + \mathbf{P}_i(t+1) \sum_{j=1}^n \{g_{ij}(t) \cdot [\mu_j(t) \mathbf{P}_j(t)]^{-1} \\ & \cdot (\vec{z}_j(t) - \vec{z}_i(t))\} \end{aligned} \quad (3)$$

$$\mu_j(t) = \sum_{k=1, k \neq j}^n g_{kj}(t) \quad (4)$$

where  $\mathbf{P}_i$  is the covariance matrix assembled using the radius basis function kernel (1) and the grid variance  $\vec{\sigma}$ ,  $\mathbf{Q}(t)$  is the process noise (used only when a vehicle becomes completely



disconnected and must complete the consensus on their own),  $\bar{z}_i$  is the agent's own information,  $g_{ij}$  is the adjacency matrix of the communication graph between agents  $\mathcal{A}_i$  and  $\mathcal{A}_j$ , and  $\mu_j(t)$  is a scaling factor associated with agent  $\mathcal{A}_j$ .

#### D. MOOS-IvP

MOOS-IvP [27] is an open source C++ robotic autonomy software mainly used for marine vehicles. It consists of two parts, MOOS and the IvP Helm, and is intended to be run as backseat autonomy. The Mission Oriented Operating Suite (MOOS) is a robotic middleware that uses a publish-subscribe structure. The various processes (MOOS apps) that run in a mission publish messages to a central database process (MOOSDB) and subscribe to publications from other processes. One of these processes is the Interval Programming (IvP) Helm, which provides behavior-based autonomy.

#### E. Proposal Based Adaptive Channel Search

Here we present our main result, a more specialized method for solving the channel identification problem, which we refer to as the Proposal Based Adaptive Channel Search (PBACS) algorithm. There are two stages to this approach: an exploratory sweep and a search along candidate paths. A simplified version of the process is illustrated in Figure 3, and the proposal algorithm is reproduced in Algorithm 1.

1) *First Stage - Exploratory Sweep:* The first stage of PBACS is an exploratory sweep of the area. Other adaptive sampling works have also employed an initial exploratory lawnmower sweep to seed the remainder of the search [14], [8]. For our problem, we can use such a sweep to help save time by eliminating areas that do not meet the necessary depth criteria, thereby directing the search toward more likely channel regions (Step 1 in Figure 3). For a single vehicle mission we set the initial sweep to cover the start area of the grid, and for a two vehicle mission we cover the start and end goal areas. The sweep area for each subsequent vehicle is an equally spaced line in between.

2) *Second Stage - Path Exploration:* The second stage after the sweep is the path exploration stage, shown in Algorithm 1. Vehicles enter this stage after they complete their initial sweep, and this transition often occurs asynchronously due to the difference in transit times to the initial sweep locations.

The goal of this stage is to identify and explore candidate paths that may still be viable. Each vehicle proposes a path between the start and goal regions that may be part of a viable channel (Step 2 in Figure 3). These candidate paths can be generated using any path planner; here we used a common variant of the A\* planner which searches for a path that connects any of several start and goal locations.

The candidate path must be clear of obstacles. Grid-cells are considered obstacles only if they have a sufficiently low variance *and* are too shallow. This way, candidate paths are made up of cells that are either certainly deep enough, or that we are uncertain about how deep they actually are.

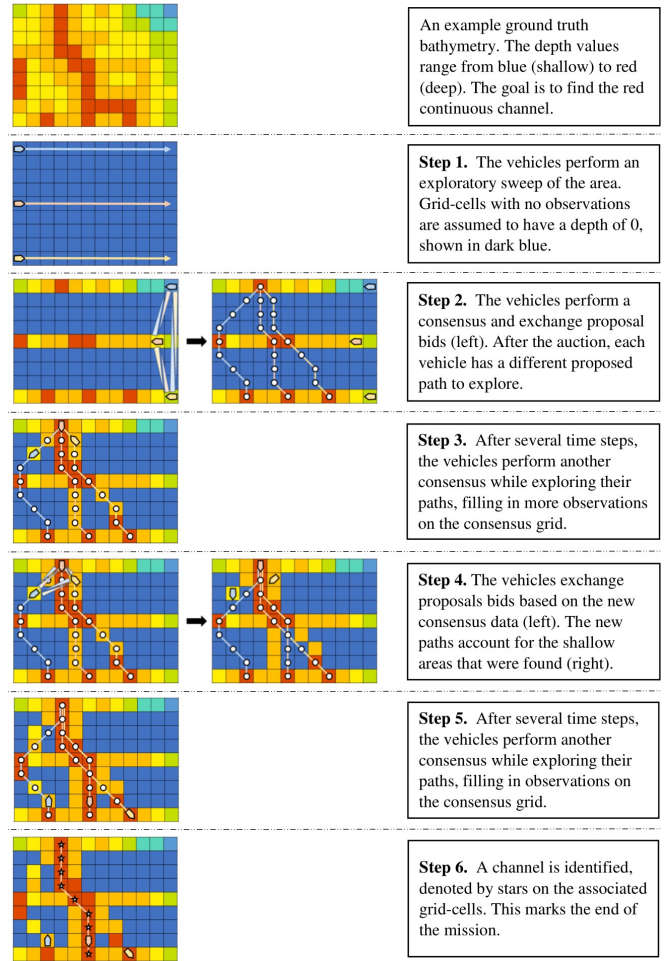


Fig. 3. The simplified steps of PBACS.

The variance threshold for considering a shallow grid-cell to be an obstacle is calculated dynamically as a percentage of the range between the current minimum and maximum variance across the grid, i.e.

$$\sigma_{th} = \sigma_{min} + \eta(\sigma_{max} - \sigma_{min}). \quad (5)$$

All grid-cells whose variance is less than  $\sigma_{th}$  *and* whose depth estimate is shallower than the desired channel depth are considered obstacles. This threshold must be set high enough to exclude shallow grid-cells with low variance, typically those that have been directly measured by at least one vehicle. The threshold should also be low enough to not exclude shallow grid-cells with high variance, typically those that were interpolated. We experimentally determined  $\eta = 0.33$  to be sufficient for both simulation and fieldwork.

Upon completion of each GPR estimate and consensus, the path is rechecked to ensure that no new obstacles were found on it, and that it is still optimal (Steps 3,4,5 in Figure 3). If a more optimal and obstacle-free path is found, the vehicle switches to this path (Step 4 in Figure 3). We periodically check for the existence of a valid continuous channel, which marks the end of the mission (Step 6 in Figure 3).

3) *Path Search Direction*: Once a vehicle has a new candidate path to explore, its first waypoint on that path is the point with the shortest Euclidean distance to its current position. Since this is most likely not an endpoint of the candidate path, we must choose the direction that the vehicle will traverse the path. The first condition we check is whether we have an unexplored endpoint. Due to the preliminary sweep stage, this condition would only happen in the single vehicle case. The second condition is checking which side of the path has a higher variance, so that the vehicle is directed toward less explored regions. This is done by comparing the sum of the variances associated with either direction, with an exponentially increasing discount factor applied to points that are further away. The direction with the higher reward is chosen. The vehicle traverses the waypoints in this direction of the path until it reaches the endpoint. If no obstacles are found, the vehicle reverses to cover the other direction. An example of direction choosing is illustrated in Figure 4.

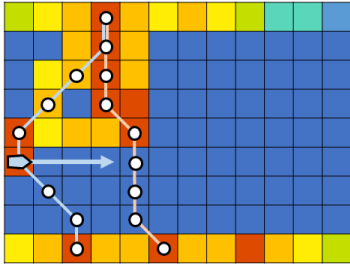


Fig. 4. An example of a vehicle switching to a new candidate path, in a mission where it aims to identify a continuous deep channel. The desired channel depth is shown in red, and areas with no samples and high variance are shown in blue. The vehicle has encountered an obstacle on  $\mathbf{p}_{curr}$ , the path it was exploring (left path), and has found  $\mathbf{p}_{prop}$ , a new candidate path (right path). The blue arrow points in the direction of  $\mathbf{p}_a$ , the vehicle's first waypoint on the new path. There are two choices of directions in which to traverse the path,  $\mathbf{p}_r$  (reverse/up) or  $\mathbf{p}_f$  (forward/down). Since  $\mathbf{p}_f$  would pass through more high variance grid-cells, this direction is chosen.

4) *Proposal Bidding*: In the multi-vehicle case, vehicles allocate viable paths among themselves by sharing their locally found path with other vehicles as a proposal with an associated cost, and checking for conflicts. When vehicles update their consensus estimate of the field, each vehicle finds the most optimal potentially viable path. The vehicle then proposes this candidate path to the other vehicles by placing a proposed bid with the cost of transiting to the path. For the cost function, we use the Euclidean distance to the closest point on the path. Each vehicle compares its own proposal to the ones it receives from the others. If there are no conflicts, the vehicle transits to this path and uses a waypoint following behavior to survey along the line. If there is a conflict, the vehicle with a lower cost bid wins. The losing vehicle must propose a new path and go through another iteration of bidding with all other vehicles that remain unassigned. The new proposal for subsequent iteration rounds takes into account the assigned paths by considering the cells in those paths to be obstacles, ensuring that new proposals do not overlap with paths assigned in the previous iteration. In the case where there are more vehicles

than there are potential paths, a vehicle with no path will revert to using an MDP-based surveying mode to explore more of the field until a path becomes available. The proposal process is repeated upon each completion of a consensus.

---

#### Algorithm 1 Pseudocode of the main PBACS algorithm

---

##### Global variables and parameters

$\sigma_{th}$	variance threshold (5)
$t_{wait}$	time to wait for other proposals
$\mathbf{p}_{curr}$	vector of waypoints of current path [ $p_1, p_2, \dots, p_N$ ]
$N_p$	number of waypoints/vertices in path $\mathbf{p}$
$\mathbf{P}$	vector of tuples ( $\mathbf{p}_i, c_i, t_i$ ) containing received proposals, costs, and time received

```

1: procedure PBACS
2:   initialize  $won \leftarrow false$ 
3:   repeat
4:     Handle incoming messages, checking for new
       consensus data and proposals
5:     if new consensus data received then
6:        $chnl\_fnd \leftarrow$  check for channel  $\triangleright A^*$ 
7:        $waited \leftarrow time\_since\_last\_prop > t_{wait}$ 
8:       if  $\neg chnl\_fnd$  and  $\neg won$  and  $waited$  then
9:          $won = CHECKPROPOSALS(\mathbf{P})$ 
10:        if  $\neg won$  then
11:           $\mathbf{p}_{new} \leftarrow$  find candidate path  $\triangleright A^*$ 
12:          if  $\mathbf{p}_{new} \neq []$  then
13:             $cond1 = \mathbf{p}_{curr}$  has new obstacles
14:             $cond2 = N_{\mathbf{p}_{curr}} > N_{\mathbf{p}_{new}}$ 
15:            if  $cond1$  or  $cond2$  then
16:               $\mathbf{p}_{prop} \leftarrow \mathbf{p}_{new}$ 
17:            else
18:               $\mathbf{p}_{prop} \leftarrow \mathbf{p}_{curr}$ 
19:            end if
20:          else
21:            exit, use MDP planning
22:          end if
23:           $c_{prop} \leftarrow$  min distance to  $\mathbf{p}_{prop}$ 
24:          send  $\mathbf{p}_{prop}$  and  $c_{prop}$  to other vehicles
25:        else if  $won$  and  $\mathbf{p}_{prop} \neq \mathbf{p}_{curr}$  then
26:           $p_a \leftarrow$  get closest waypoint in  $\mathbf{p}_{prop}$ 
27:           $\mathbf{p}_{curr} = GETDIRECTION(\mathbf{p}_{prop}, p_a)$ 
28:          publish  $\mathbf{p}_{curr}$  to waypoint behavior
29:        end if
30:      end if
31:    end if
32:  until  $channel\_found$ 
33: end procedure

```

---

#### F. Existing Methods for Comparison

1) *Lawnmower Survey*: The most common method of surveying a region is with a lawnmower pattern, also referred to as a boustrophedon in coverage path planning [28]. However, the success of lawnmower surveys in quickly identifying a channel is highly dependent on the (lucky) choice of starting

locations and distributions of vehicles that fit the underlying map. In this work, we are interested in approaches that do not rely on luck and perform better in aggregate.

2) *Markov decision processes*: We can formulate the problem as an MDP [29]. An MDP consists of the following: a set of states  $S$  with an initial state  $s_0$ , a set of actions in each state  $A$ , a transition model  $P(s'|s, a)$  giving the probability that an action  $a$  in state  $s$  will lead to state  $s'$ , and a reward function  $R(s)$ .

A solution to the MDP is in the form of a policy  $\pi$ , where  $\pi(s)$  gives the recommended action at state  $s$ . The optimal policy for a state  $\pi^*(s)$  is given by:

$$\pi^*(s) = \operatorname{argmax}_{a \in A(s)} \sum_{s'} P(s'|s, a) U(s') \quad (6)$$

where  $U(s)$  is a utility function. This utility function can be estimated using value iteration, which is computed by iteratively applying a Bellman update.

For our implementation, we define the root state to be the grid-cell corresponding to the vehicle's current position and heading. For the actions, to account for the underactuated vehicle's maneuverability, we define three possible next grid-cells based on the vehicle's heading: ahead, ahead-left, or ahead-right. These heading-based grid-cell choices are shown in Figure 5 below. If the action is to maintain heading, meaning transiting to the cell straight ahead, the probability is 0.82 that this state transition is achieved. The probability that the vehicle turns and goes ahead-left or ahead-right instead is 0.09 for each turn. If the action is to change heading, meaning transiting to the ahead-left or ahead-right cell, the probability that this is achieved is 0.7. The probability that the vehicle maintains heading instead is 0.2, and the probability of turning the other direction is 0.1. These probabilities are normalized based on the total probability of all feasible actions.

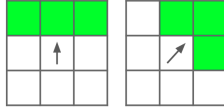


Fig. 5. Examples of possible neighbor cells to which a vehicle can transit are highlighted based on current heading, represented by an arrow direction.

An MDP can be implemented with different reward functions. We compare the performance of two different functions, UCB and MVI. UCB as a reward criterion is a common, state-of-the-art choice in online decision making [30] [31]. An alternative to UCB reward calculation is MVI, defined by Flaspohler et al. [9], based on the Max-value Entropy Search (MES) criterion defined by Wang et al. [10]. As shown by Flaspohler et al., over time the MVI reward converges to the global maximum, while UCB rewards high-value regions more uniformly.

Due to computational constraints of fieldwork hardware, we implement the MDP as a myopic planner with a limited look-ahead depth. Based on this information, the vehicle determines the current optimal path to take. The utility function is recalculated once it reaches the next grid-cell.

## IV. RESULTS

### A. Simulation Experiments

To test algorithm performance in simulation, we generated six possible bathymetry scenario files. For non-symmetric bathymetry configurations, we also used mirrored versions to check for biases that different orientations can introduce. Including these mirrored versions, we tested a total of ten scenarios. The ten bathymetry scenarios are shown in Figure 6 below. Each area represents a 500 meter by 750 meter rectangle with 20 meter by 20 meter grid-cells. The grids are tilted to represent the path planning algorithms not being dependent on a perfectly horizontal or vertical grid, to account for possible shoreline bounds. The depth values over all scenarios range from 6 feet to 26 feet.

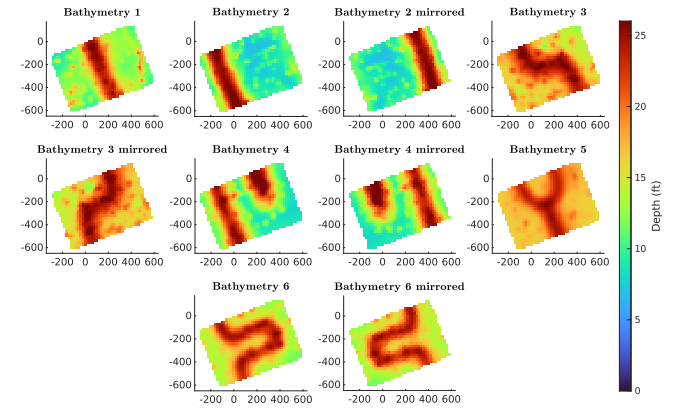


Fig. 6. The ten bathymetry grid scenarios for simulation testing. The x and y axis markers represent distances in meters.

We define the depth threshold to be 20 feet. Each vehicle's speed is set to 2.4 m/s. For the two MDP approaches, we use a look-ahead depth of 6 cells, recalculated every time a vehicle enters a cell.

1) *Simulation Results*: We only provide a general summary of performance due to page length constraints. Detailed results from each scenario can be found in [32].

In general, the PBACS algorithm performs better than the lawnmower survey pattern. As shown in Figure 7, the PBACS mission durations are shorter than the lawnmower mission durations on average, but there are some outlier cases of long PBACS missions. The single vehicle case of PBACS times out or is close to timing out for the very curved channel in the Bathymetry 6 scenario and for one orientation of the "dead end" channel in the Bathymetry 4 scenario. The two vehicle case of PBACS also has a long mission duration for the Bathymetry 6 scenario. The three and four vehicle cases of PBACS consistently perform better than the three and four vehicle lawnmower surveys, except when a vehicle's lawnmower start location aligns with a straight channel.

Overall, the results shown here indicate that the optimal amount of vehicles for the scenarios used here is three when using PBACS. Using three vehicles avoids the possible long mission durations of the one and two vehicle cases. Adding a fourth vehicle does not offer much improvement in mission

duration, and could potentially slightly increase it as well. These numbers are based on a maximum of one bend in the channel (scenario 6). If more bends were to be added, it is possible that four or more vehicles would be optimal instead.

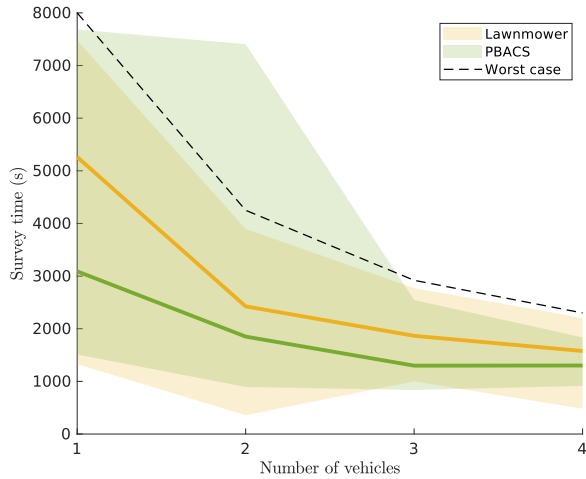


Fig. 7. Means and ranges of mission times across all 10 simulated bathymetry scenarios for the lawnmower and PBACS approaches. For each vehicle number, there are 10 lawnmower data points and 50 PBACS data points. The dashed black line shows the duration of a theoretical mission where the lawnmower covers the entire field. This is not linear due to the field not being evenly divisible by all of the vehicle amounts, and to account for consensus times.

### B. Field Experiments

From April to June 2022, we performed fieldwork trials of the four path planning approaches on the Charles River near the MIT Sailing Pavilion. There were two sets of fieldwork trials. We first performed a comparison study of the four methods in a section of the river adjacent the MIT Sailing Pavilion. The details of these experiments are provided in the remainder of this section. We also repeatedly demonstrated the performance of the PBACS approach to quickly identify the well-defined channel that was dredged in the Charles River on the side opposite the MIT Sailing Pavilion. The results of these demonstrations are shown in Figure 1.

For the comparison study, the survey area is a 170 meter by 260 meter rectangular grid, with 10 meter by 10 meter grid-cells. This area, chosen for its proximity to the lab space, does not have a clearly defined channel. However, it contains some straight paths down through deep areas as well as curved paths.

1) *Field Results:* In this section, we describe the results of 28 comparison field trials. As in the simulations, the results for the lawnmower survey are taken from one run. The results of the PBACS algorithm are taken from four runs of each vehicle number. We only have data for the two and three vehicle cases of both MDP approaches; these results are taken from two runs each.

Figures 8 and 9 below show the mission times and paths found. The ground truth grid displayed in Figure 9 was averaged from three complete lawnmower surveys, but there

is still some variability,  $\pm 1$  foot, in the water level and surface conditions of each field mission. This would account for some of the paths passing through grid-cells that appear shallow on the plotted grid.

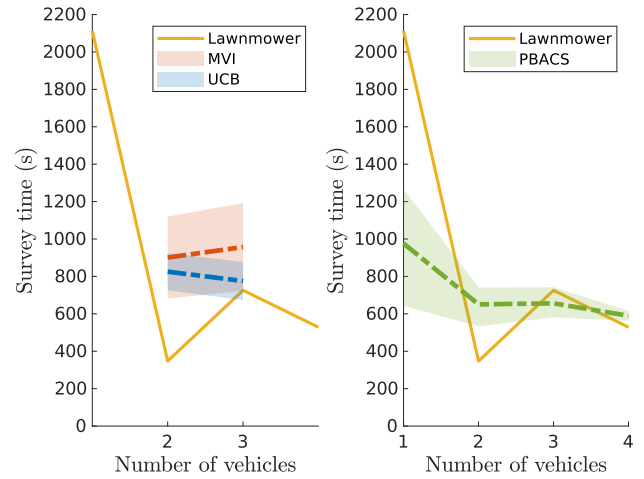


Fig. 8. Field mission time ranges for the MDP and PBACS. The means are marked with dashed lines.

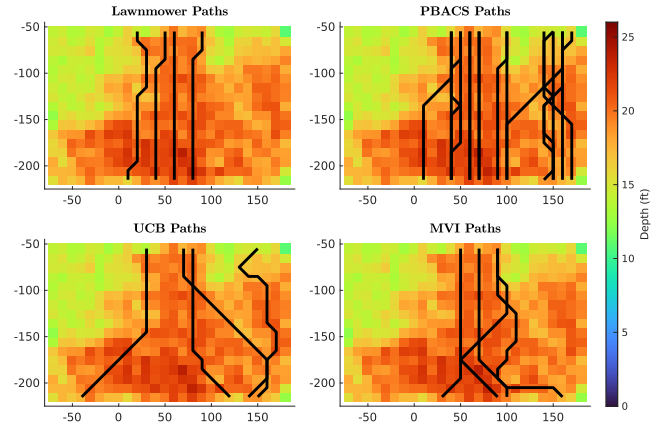


Fig. 9. All final paths found during field missions, separated by path planning approach. The x and y axis markers represent distances in meters.

The PBACS mission duration decreases when the number of vehicles is increased, as does the variation in the mission time. As was found in simulations, when a relatively straight channel path exists, the largest improvement in time comes from increasing the vehicle amount from one to two.

Because the channel is less defined in our field area than it is in the simulation scenarios, there is more variation between approaches in the types of paths found. In all of the simulation runs, the channel paths are all concentrated in the same general areas and have the same general shapes. Here, the lawnmower survey and PBACS both have generally straighter paths than the two MDP approaches, since the lawnmower survey runs parallel to this direction and since PBACS checks for the shortest straight paths first.



## V. CONCLUSIONS

To the best of our knowledge, this paper describes the first formal investigation into the rapid channel identification problem. The rapid channel identification problem is well suited to the use of adaptive sampling. However, our results suggest that the problem requires fundamentally different approaches than those used in other adaptive sampling problems. Through our simulation testing and field testing with USVs and single beam altimeters, we found that the PBACS algorithm generally outperforms the lawnmower and both MDP reward functions in multi-vehicle cases. There are some exceptions, namely when the lawnmower survey start is aligned with a straight channel. Another notable exception is when the channel is very curved. In this case, a two vehicle mission may have poor performance, but on average three and four vehicle PBACS missions were still faster than three and four lawnmower or MDP missions.

Potential areas of improvement for the PBACS algorithm include implementing a more sophisticated auction-based approach to allocating proposed paths among vehicles. Another potential improvement is extending the proposal cost function beyond the Euclidean distance, perhaps including penalties for heading changes.

## REFERENCES

- [1] 2017. [Online]. Available: <https://mit.sea-grant.net/maps/charleschart/>
- [2] C. E. Rasmussen and C. K. I. Williams, *Gaussian Processes for Machine Learning (Adaptive Computation and Machine Learning)*. The MIT Press, 2005.
- [3] G. E. Berget, T. O. Fossum, T. A. Johansen, J. Eidsvik, and K. Rajan, "Adaptive sampling of ocean processes using an AUV with a Gaussian proxy model," *IFAC-PapersOnLine*, vol. 51, no. 29, pp. 238–243, 2018, 11th IFAC Conference on Control Applications in Marine Systems, Robotics, and Vehicles CAMS 2018.
- [4] T. Fossum, G. Fragoso, E. Davies, J. Ullgren, R. Mendes, G. Johnsen, I. Ellingsen, J. Eidsvik, M. Ludvigsen, and K. Rajan, "Toward adaptive robotic sampling of phytoplankton in the coastal ocean," *Science Robotics*, vol. 4, p. eaav3041, 02 2019.
- [5] S. Yan, Y. Li, X. Feng, S. Li, Y. Tang, Z. Li, and M. Yuan, "An AUV adaptive sampling path planning method based on online model prediction," *IFAC-PapersOnLine*, vol. 52, no. 21, pp. 323–328, 2019, 12th IFAC Conference on Control Applications in Marine Systems, Robotics, and Vehicles CAMS 2019.
- [6] P. Stankiewicz, Y. T. Tan, and M. Kobilarov, "Adaptive sampling with an autonomous underwater vehicle in static marine environments," *Journal of Field Robotics*, vol. 38, no. 4, pp. 572–597, 2021.
- [7] B. Bayat, N. Crasta, A. Crespi, A. M. Pascoal, and A. Ijspeert, "Environmental monitoring using autonomous vehicles: a survey of recent searching techniques," *Current Opinion in Biotechnology*, vol. 45, pp. 76–84, 2017.
- [8] C. Paliotta, D. Belleter, and K. Pettersen, "Adaptive source seeking with leader-follower formation control," *IFAC-PapersOnLine*, vol. 48, pp. 285–290, 12 2015.
- [9] G. Flaspohler, V. Preston, A. P. M. Michel, Y. Girdhar, and N. Roy, "Information-guided robotic maximum seek-and-sample in partially observable continuous environments," *IEEE Robotics and Automation Letters*, vol. 4, no. 4, pp. 3782–3789, 2019.
- [10] Z. Wang and S. Jegelka, "Max-value entropy search for efficient bayesian optimization," in *Proceedings of the 34th International Conference on Machine Learning - Volume 70*, ser. ICML'17. JMLR.org, 2017, p. 3627–3635.
- [11] Y. Zhang, M. Godin, J. G. Bellingham, and J. P. Ryan, "Ocean front detection and tracking by an autonomous underwater vehicle," in *OCEANS'11 MTS/IEEE KONA*, 2011, pp. 1–4.
- [12] S. Petillo, H. Schmidt, P. Lermusiaux, D. Yoerger, and A. Balasuriya, "Autonomous and adaptive oceanographic front tracking on board autonomous underwater vehicles," in *OCEANS 2015 - Genova*, 2015, pp. 1–10.
- [13] E. Fiorelli, N. E. Leonard, P. Bhatta, D. A. Paley, R. Bachmayer, and D. M. Fratantoni, "Multi-AUV control and adaptive sampling in monterey bay," *IEEE Journal of Oceanic Engineering*, vol. 31, no. 4, pp. 935–948, 2006.
- [14] A. Bennett and J. Leonard, "A behavior-based approach to adaptive feature detection and following with autonomous underwater vehicles," *IEEE Journal of Oceanic Engineering*, vol. 25, no. 2, pp. 213–226, 2000.
- [15] A. Khoshrou, A. P. Aguiar, and F. Pereira, "Adaptive sampling using an unsupervised learning of GMMs applied to a fleet of AUVs with CTD measurements," in *Robot 2015: Second Iberian Robotics Conference*, 11 2015.
- [16] S. Kemna, J. G. Rogers, C. Nieto-Granda, S. Young, and G. S. Sukhatme, "Multi-robot coordination through dynamic Voronoi partitioning for informative adaptive sampling in communication-constrained environments," in *2017 IEEE International Conference on Robotics and Automation (ICRA)*, 2017, pp. 2124–2130.
- [17] M. Alighanbari and J. How, "Decentralized task assignment for unmanned aerial vehicles," in *Proceedings of the 44th IEEE Conference on Decision and Control*, 2005, pp. 5668–5673.
- [18] W. Ren, R. Beard, and E. Atkins, "A survey of consensus problems in multi-agent coordination," in *Proceedings of the 2005, American Control Conference, 2005.*, 2005, pp. 1859–1864 vol. 3.
- [19] W. Ren, R. Beard, and D. Kingston, "Multi-agent Kalman consensus with relative uncertainty," in *Proceedings of the 2005, American Control Conference, 2005.*, 2005, pp. 1865–1870 vol. 3.
- [20] M. Alighanbari and J. How, "An unbiased Kalman consensus algorithm," in *2006 American Control Conference*, 2006, pp. 6 pp.–.
- [21] D. Bertsekas, "Auction algorithms for network flow problems: A tutorial introduction," *Computational Optimization and Applications*, vol. 1, no. 1, pp. 7–66, Oct. 1992, copyright: Copyright 2007 Elsevier B.V., All rights reserved.
- [22] N. Michael, M. M. Zavlanos, V. Kumar, and G. J. Pappas, "Distributed multi-robot task assignment and formation control," in *2008 IEEE International Conference on Robotics and Automation*, 2008, pp. 128–133.
- [23] M. M. Zavlanos, L. Spesivtsev, and G. J. Pappas, "A distributed auction algorithm for the assignment problem," in *2008 47th IEEE Conference on Decision and Control*, 2008, pp. 1212–1217.
- [24] L. Brunet, H.-L. Choi, and J. How, "Consensus-based auction approaches for decentralized task assignment," in *AIAA guidance, navigation and control conference and exhibit*, 2008, p. 6839.
- [25] S. Raja, G. Habibi, and J. P. How, "Communication-aware consensus-based decentralized task allocation in communication constrained environments," *IEEE Access*, vol. 10, pp. 19 753–19 767, 2021.
- [26] S. Das, S. Roy, and R. Sambasivan, "Fast Gaussian process regression for big data," *Big Data Research*, vol. 14, pp. 12–26, 2018.
- [27] M. R. Benjamin, H. Schmidt, P. Newman, and J. J. Leonard, "Nested autonomy for unmanned marine vehicles with MOOS-IvP," *J. Field Robotics*, vol. 27, pp. 834–875, 2010.
- [28] H. Choset and P. Pignon, "Coverage path planning: The boustrophedon cellular decomposition," in *Field and Service Robotics*, A. Zelinsky, Ed. London: Springer London, 1998, pp. 203–209.
- [29] R. Bellman, "A Markovian Decision Process," *Indiana University Mathematics Journal*, vol. 6, pp. 679–684, 1957.
- [30] N. Srinivas, A. Krause, S. M. Kakade, and M. W. Seeger, "Information-theoretic regret bounds for Gaussian process optimization in the bandit setting," *IEEE Transactions on Information Theory*, vol. 58, no. 5, pp. 3250–3265, 2012.
- [31] W. Sun, N. Sood, D. Dey, G. Ranade, S. Prakash, and A. Kapoor, "No-regret replanning under uncertainty," in *2017 IEEE International Conference on Robotics and Automation (ICRA)*. IEEE, 2017, pp. 6420–6427.
- [32] N. Gershfeld, "Adaptive collaborative channel finding approaches for autonomous marine vehicles," Master's thesis, Massachusetts Institute of Technology, Cambridge, MA, 2022.